Local magnetic anisotropy in $BaFe_2As_2$: a polarized inelastic neutron scattering study

N. Qureshi,[1,*] P. Steffens,[2] S. Wurmehl,[3] S. Aswartham,[3] B. Büchner,[3] and M. Braden[1,†]

[1] *II. Physikalisches Institut, Universität zu Köln, Zülpicher Strasse 77, D-50937 Köln, Germany*
[2] *Institut Max von Laue-Paul Langevin, 6 rue Jules Horowitz, BP 156, 38042 Grenoble Cedex 9, France*
[3] *Leibniz-Institut für Festkörper- und Werkstoffforschung (IFW) Dresden, D-01171 Dresden, Germany*

(Dated: January 12, 2012)

The anisotropy of the magnetic excitations in $BaFe_2As_2$ was studied by polarized inelastic neutron scattering which allows one to separate the components of the magnetic response. Despite the in-plane orientation of the static ordered moment we find the in-plane polarized magnons to exhibit a larger gap than the out-of-plane polarized ones indicating very strong single-ion anisotropy within the layers. It costs more energy to rotate a spin within the orthorhombic *a*-*b* plane than rotating it perpendicular to the FeAs layers.

PACS numbers: 61.50.Ks; 74.70.Xa; 75.30.Fv
Keywords:

The recent discovery of the iron-based oxypnictide superconductors[1] has triggered enormous activity exploring the superconducting pairing mechanism in these materials. Density functional theory (DFT) calculations[2,3] indicate that the conventional electron-phonon coupling is by far too weak in the iron pnictides to account for the observed high critical temperatures of up to $T_c = 55K$ (Ref. 4). Instead, the phase diagrams of many FeAs-based families suggest a magnetic pairing mechanism, as superconductivity appears close to an antiferromagnetic spin-density wave (SDW) phase.[5–7] Superconductivity can even coexist with the SDW order parameter which then slightly decreases upon entering the superconducting state.[8–10] Furthermore, the onset of superconductivity in doped $BaFe_2As_2$ compounds is accompanied by the appearance of additional magnetic scattering at the SDW wave vector.[11–13]

$BaFe_2As_2$ becomes superconducting on hole-doping,[7] on electron-doping[14] or by the application of pressure.[15,16] Pure $BaFe_2As_2$ exhibits a structural phase transition from the high-temperature tetragonal ($I4/mmm$) to the low-temperature orthorhombic phase ($Fmmm$), see Fig. 1(a), at T_S ∼140 K (Ref. 17) accompanied by a magnetic phase transition into a collinear antiferromagnetic structure with an ordered Fe moment of 0.87 μ_B (Ref. 17). This orthorhombic antiferromagnetic phase exhibits remarkable properties. The magnetic structure shown in Fig. 1(b) breaks tetragonal symmetry, one may therefore expect some orthorhombic splitting in the crystal structure as it indeed occurs, but this splitting remains rather small. However, the signature of the orthorhombic structure in the electronic properties is much stronger than the small orthorhombic splitting in the lattice constants would suggest. Resistivity measurements on detwinned single crystals reveal pronounced anisotropy associated already with the precursors of the orthorhombic phase.[18] The observation of a larger resistivity along the shorter axis with ferromagnetic spin coupling is further surprising. Also scanning tunnelling microscopy[19] and optical conductivity analyses[20] report essential in-plane anisotropy. Magnon excitations in the SDW phase have been studied by several inelastic neutron scattering experiments (unpolarized) and, again, the slope of the low energy dispersion is anisotropic.[21–24] The nearest neighbor interaction along the *a* and *b* directions needed to model the magnon dispersion even show opposite signs. This remarkable anisotropy in magnetic exchange, however, can qualitatively be explained by DFT.[25] The pronounced anisotropies in the electronic properties inspired a model of orbital polarization[26] which gets support from recent ARPES experiments,[27,28] as well as speculations about the role of nematic properties.

In this work we analyze the magnetic single-ion anisotropy which can be deduced from the gap in the magnetic excitations finding again remarkably strong in-plane anisotropy. It costs more energy to rotate the spin within the FeAs layers than aligning it perpendicular to them, in contrast to the simple expectation of an easy-plane system.

Large $BaFe_2As_2$ single crystals were obtained by a self-flux technique.[29] The pre-reacted precursor materi-

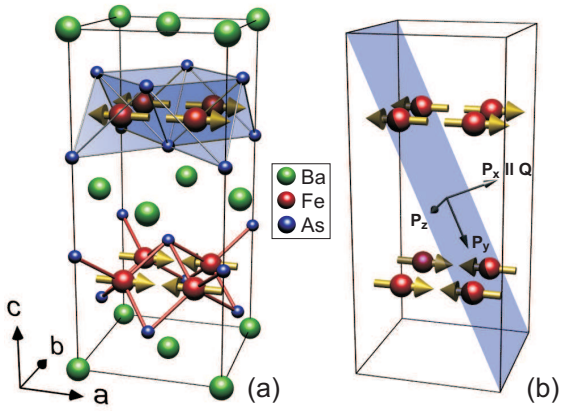

FIG. 1: (Color online) (a) Visualization of the crystal and magnetic structure of $BaFe_2As_2$ in the orthorhombic setting. (b) Definition of the reference frame for the neutron polarization analysis on the (1 0 1) reflection as an example (only the Fe ions are depicted in the unit cell).

als FeAs, Fe_2As, Co_2As and BaAs were mixed leading to a $Ba(Fe, Co)_{3.1}As_{3.1}$ composition. This composition was used to achieve a homogeneous melt at T = 1463 K. The melt was cooled slowly under a temperature gradient in a double-wall crucible assembly to obtain large and flux-free single crystals of $BaFe_2As_2$. Using this technique, single crystals with lateral dimensions up to 25 x 10 mm^2 and thickness up to 1 mm were obtained. Two plate-like single crystals with masses of 804 mg and 200 mg have been coaligned in order to decrease counting time. The experiment has been carried out at the thermal-beam three-axis spectrometer IN20 (ILL) using polarizing Heusler (111) crystals as monochromator and as analyzer. Longitudinal polarization analysis was performed with a set of Helmholtz coils to guide and orient the neutron polarization. The longitudinal polarization analysis permits separating the nuclear cross-section and the individual components of the magnetic cross-section into the spin-flip (SF) and non-spin-flip (NSF) channels by selecting the initial and the final polarization direction of the neutrons. We use the conventional reference frame for polarization analysis,[30] see Fig. 1(b), with the x axis parallel to the scattering vector $\mathbf{Q}$, y perpendicular to x within the scattering plane, and z perpendicular to x and y (perpendicular to the scattering plane). The sample has been mounted in the [100]/[001] scattering geometry in orthorhombic notation, but note that the crystal is twinned so that part of the crystal is in [010]/[001] geometry and signals from both parts superpose.

Longitudinal polarization analysis adds additional selection rules to the general law in neutron scattering that only magnetic components perpendicular to the scattering vector contribute. Only the magnetic components perpendicular to the axis of polarization analysis contribute to the SF scattering whereas the parallel components contribute to the NSF scattering.[30] Nuclear scattering is always a NSF process. We measured the NSF cross-section for polarization parallel to x, serving as a reference for eventual contaminations, and all three SF cross-sections keeping $\mathbf{k}_f$ constant. Applying a correction for the finite flipping ratio of $R = 7.4$ the magnetic cross-sections σ_y and σ_z (Eqs. 1 and 2) as well as the background in the SF channel (Eq. 3) can be calculated according to:

$$\sigma_y = \frac{R+1}{R-1}[I(SF_x) - I(SF_y)]), \quad (1)$$

$$\sigma_z = \frac{R+1}{R-1}[I(SF_x) - I(SF_z)], \quad (2)$$

$$BGR_{SF}(R) = \frac{R}{R-1}[I(SF_y) + I(SF_z)] - \frac{R+1}{R-1}I(SF_x). \quad (3)$$

In Fig. 2 the maximum intensity of the magnetic (1 0 1) reflection is shown as a function of temperature for the two channels. A power law has been fitted to the σ_y data revealing a T_N of approximately 137 K. The entire elastic signal is found in σ_y (σ_z is essentially zero) in perfect agreement with the well-accepted magnetic structure shown in Fig. 1 with moments parallel to the a axis.

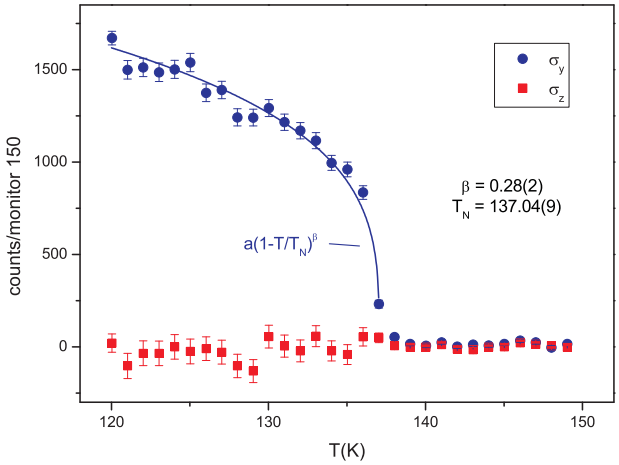

FIG. 2: (Color online) Temperature dependence of the elastic magnetic scattering cross section at $\mathbf{Q}$=(1 0 1) revealing that almost the entire magnetic signal stems from σ_y. The values have been obtained by Eqs. 1 and 2. The fitting of a power law to the σ_y data yields a Néel temperature of 137 K.

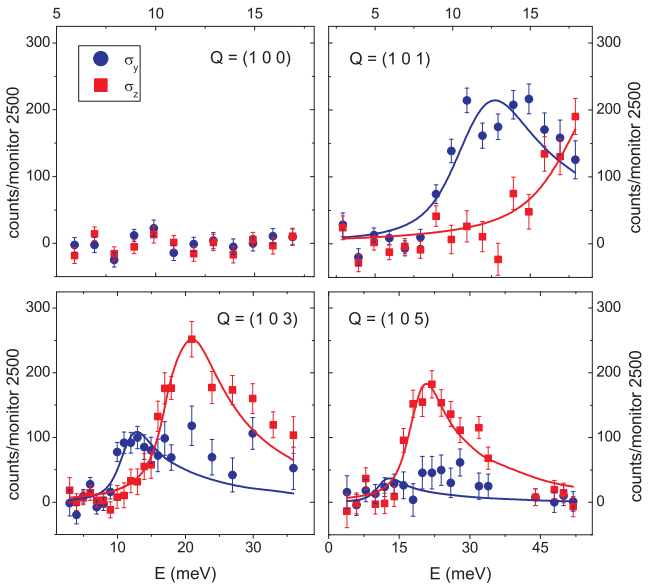

FIG. 3: (Color online) Inelastic constant-$\mathbf{Q}$ scans at the magnetic Brillouin-zone centers (1 0 l) for different l values and at (1 0 0). (Blue) dots represent the magnetic scattering cross section σ_y, while (red) squares depict σ_z. The cross sections have been obtained by measuring the SF_z and SF_y channels, respectively, and applying Eqs. 1 and 2. The solid lines are spline-interpolated spin-wave theory calculations folded with the experimental resolution.

Inelastic constant $\mathbf{Q}$-scans were performed at the magnetic zone centers $\mathbf{Q}$=(1 0 l) with l=1,3 and 5, and at $\mathbf{Q}$=(1 0 0) which is a magnetic zone boundary due to the finite interlayer coupling (Fig. 3). The scan at $\mathbf{Q}$=(1 0 0) does not indicate any magnetic scattering in agreement with the published magnon dispersion for

$CaFe_2As_2$ (Refs. 21,22) and for $SrFe_2As_2$ (Refs. 23,24) indicating energies of the order of 100 meV for this **q** value. Due to the high zone-boundary energies the magnetic signals of the differently oriented twin domains do not superimpose in the scans at **Q**=(1 0 l) with l=1,3 and 5, which are zone boundaries for the second domain orientation. The magnetic-zone-center scans sense the gap of the magnon dispersion arising from anisotropy. For a system with uniaxial anisotropy one expects a single gap for the two still degenerate transversally polarized magnons. This degeneracy, however, lifts for orthorhombic local symmetry causing an easy, a medium and a hard axis.[31] We will see that such orthorhombic single-ion anisotropy is needed to describe magnetic excitations in $BaFe_2As_2$. The cross sections σ_y and σ_z unambiguously show the splitting of the zone-center magnons in $BaFe_2As_2$. The z direction of our reference system is always parallel to the b direction and therefore σ_z measures the transverse magnon polarized along the b direction. The y direction lies always in the $a^\star$,$c^\star$ plane but rotates with varying Q_l. Since the ordered moment is parallel to a, σ_y contains only the transverse magnon polarized along the c direction (see below for discussion of the contribution of the longitudinal magnon). Due to the geometry this signal is reduced by a factor 0.92, 0.61, and 0.42 for Q_l=1,3, and 5, respectively. The qualitative analysis of the scans at the magnon zone centers immediately shows that the in-plane magnon gap is larger than the out-of-plane one. This is remarkable in view of the in-plane orientation of the ordered moment.[17] Starting from the tetragonal symmetry at high temperature one might describe $BaFe_2As_2$ as an easy-plane system similar to many layered magnets with K_2NiF_4 (214) structure, e.g. K_2FeF_4 (Ref. 32). In such a system the two transverse magnons still split as a higher-order cubic in-plane anisotropy adds to the dominating easy-plane anisotropy. There is no mass-less Goldstone mode in such system. But in this case the energy of the in-plane polarized transverse magnon is below that of the out-of-plane one.[32] The fact that $BaFe_2As_2$ exhibits the opposite behavior, the out-of-plane mode lies around 10 meV below the in-plane mode near 20 meV, excludes the description of the magnetic phase in an adapted tetragonal model, which, however, works very well for many 214-materials. The local single-ion anisotropy of the SDW phase in $BaFe_2As_2$ is truly orthorhombic.[31] This observation is in line with the strong electronic signatures[18–20] in this phase which contrast with the only weak orthorhombic splitting of the lattice. The strong single-ion anisotropy within the FeAs-layers gives strong support for pronounced orbital polarization. Previous unpolarized neutron scattering experiments on $SrFe_2As_2$, $CaFe_2As_2$ and $BaFe_2As_2$ (Ref. 33) most likely reported only on the lower gap as the different polarizations could not be resolved.

In order to quantitatively analyze the scattering distribution we have folded the experimental resolution with the scattering function of the magnon contribution using the Reslib code.[34] The dispersion and the structure factors of the magnons of the AFe_2As_2 compounds have been calculated in linear spin-wave theory by Yao and Carlson[35] for the Hamiltonian including nearest-neighbor exchange coupling along a and b directions, J_a and J_b, next-nearest neighbor exchange, J_2, inter-layer coupling, J_c, and anisotropy terms. A gap at the magnetic zone center appears only for a finite single-ion anisotropy term $\sum_i -\Lambda(S_i^z)^2$ where, in our case, Λ is equal[36] to Λ_b or Λ_c and S_i^z is the component of the spin operator of spin i in the direction of the ordered moment. Yao and Carlson obtain for the gap at the magnetic zone center: $\Delta = 2S\sqrt{\Lambda \cdot (2J_a + 4J_2 + \Lambda + 2J_c)}$. For the exchange parameters we have used the values recently determined for $SrFe_2As_2$ (Ref. 23) but normalized them to the value S=$\frac{1}{2}$·0.87 corresponding to the ordered moment in $BaFe_2As_2$, note that the full shape of the dispersion is not essential for our analysis as we only sense the low-energy part of it in our measurement. With S=$\frac{1}{2}\cdot 0.87$, SJ_{1a}=30.8 meV, SJ_{1b}=-5 meV, SJ_2=21.7 meV, SJ_c=2.3 meV, Λ_b=0.99(2) meV, and Λ_c=0.38(1) meV, we may simultaneously describe the two channels measured at the three zone centers, with the anisotropy terms and the scale factors as the only free parameters. This description takes into account the Q-dependence of the magnetic scattering due to the form factor and the geometrical factor given above. The calculated values have been interpolated with a B-spline in order to obtain continuous curves which are depicted as solid lines in Fig. 3. The perfect description of the experimental data validates the assumption that the total magnetic scattering arises from the transversally polarized magnons. Using the obtained anisotropy values we determine the in-plane and the out-of-plane gap to amount to 16.4 meV and 10.1 meV, respectively.

The single-ion anisotropy parameters obtained in our experiment can be compared to the result of relativistic DFT calculations including spin-orbit coupling;[37] the authors find that only 0.16 meV/Fe are necessary to turn the magnetic moment from the easy axis to the b direction, but that 0.20 meV/Fe are required to turn the moment perpendicular to the plane. These calculations cannot properly describe the local single-ion anisotropy in $BaFe_2As_2$ as the sign of the anisotropy does not agree with the experimental values. DFT[37] thus misses something in the description of the local symmetry of the SDW phase in $BaFe_2As_2$.

In an itinerant system with non-saturated ordered moments, one may expect a longitudinal magnetic excitation, i.e. a magnon polarized along the ordered moment. This mode contributes to the σ_y channel, but by comparing the different **Q**-values studied we can fully rule out such an interpretation for the studied energy ranges. The longitudinal contribution should increase with increasing l component, but the experimental data show the opposite and are well described by the geometry factors for the transverse mode. We can thus excude a longitudinal excitation below ∼35 meV in agreement with DFT studies predicting them at significantly higher energies.[38,39]

The temperature dependent measurement of the two magnetic cross sections at an energy transfer of 10 meV

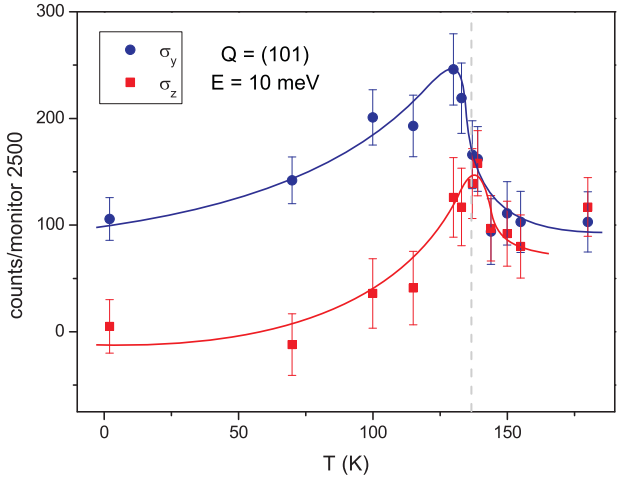

FIG. 4: (Color online) Temperature dependence of the inelastic magnetic scattering at **Q**=(1 0 1) and an energy transfer of 10 meV documenting the transition from isotropic to anisotropic fluctuations at T_N. The solid lines serve as a guide to the eye.

illustrates how the isotropic magnetic fluctuations in the paramagnetic phase transform into the anisotropic magnons below the Néel temperature (Fig. 4). There is no difference visible between the two channels at high temperature. Upon approaching the magnetic transition the intensity increases due to the softening of the magnetic response. Below the transition, the magnetic signal is almost completely suppressed in the σ_z channel where the larger gap develops, but there is only moderate reduction in the σ_y channel, where the energy transfer of 10 meV is just slightly below the low-temperature maximum.

In conclusion the polarized inelastic neutron scattering studies on the magnetic excitations in $BaFe_2As_2$ reveal a strong in-plane single-ion anisotropy which contrasts with the small structural orthorhombic distortion in this material. This pronounced local anisotropy corroborates the strong electronic signatures of the orthorhombic phase and gives further support for an important role of orbital degrees of freedom in the iron pnictides. The local anisotropy of Fe in the SDW phase apparently is insufficiently described in DFT theory even when including spin-orbit coupling.

Acknowledgments

This work was supported by the Deutsche Forschungsgemeinschaft through the Sonderforschungsbereich 608, through the Forschergruppe 538 (grant (BU887/4)), as well as through grant BE1749/12 and BE1749/13. S. Wurmehl acknowledges support by DFG under the Emmy-Noether program (Grant No. WU595/3-1). We thank M. Deutschmann, S. Pichl, K. Leger and S. Gass for technical support and A. Yaresko for the discussion about the DFT calculations.

* Electronic address: qureshi@ph2.uni-koeln.de
† Electronic address: braden@ph2.uni-koeln.de

1 Y. Kamihara et al., J. Am. Chem. Soc. **130**, 3296 (2008).
2 L. Boeri et al., Phys. Rev. Lett. **101**, 026403 (2008).
3 K. Haule et al., Phys. Rev. Lett. **100**, 226402 (2008).
4 Z. A. Ren et al., Chin. Phys. Lett **25**, 2215 (2008).
5 J. Zhao et al., Nature Mater. **7**, 953 (2008).
6 H. Luetkens et al., Nature Materials **8**, 305 (2009).
7 M. Rotter, M. Tegel, and D. Johrendt, Phys. Rev. Lett. **101**, 107006 (2008).
8 D. K. Pratt et al., Phys. Rev. Lett. **103**, 087001 (2009).
9 S. Nandi et al., Phys. Rev. Lett. **104**, 057006 (2010).
10 E. Wiesenmayer, Phys. Rev. Lett. **107**, 237001 (2010).
11 A. D. Christianson et al., arXiv 0805.0316.
12 M. D. Lumsden et al., Phys. Rev. Lett. **102**, 107005 (2009).
13 S. Chi et al., Phys. Rev. Lett. **102**, 107006 (2009).
14 A. S. Sefat, M. A. McGuire, R. Jin, B. C. Sales, and D. Mandurs, Phys. Rev. Lett. **101**, 117004 (2008).
15 M. S. Torikachvili et al., Phys. Rev. Lett. **101**, 057006 (2008).
16 P. Alireza et al., J. Phys.: Condens. Matter **21**, 012208 (2009).
17 Q. Huang et al., Phys. Rev. Lett. **101**, 257003 (2008).
18 J. H. Chu et al., Science **329**, 824 (2010).
19 T.-M. Chuang et al., Science **327**, 181 (2010).
20 M. Nakajima et al., arXiv1106.4967.
21 S. O. Diallo et al., Phys. Rev. Lett. **102**, 187206 (2009)
22 J. Zhao et al., Nature Phys. **5**, 555 (2009).
23 J. Zhao et al., Phys. Rev. Lett. **101**, 167203 (2008).
24 R. Ewings et al., Phys. Rev. B **83**, 214519 (2011).
25 M. J. Han et al., Phys. Rev. Lett. **102**, 107003 (2010).
26 C.-C. Lee et al. Phys. Rev. Lett. **103**, 267001 (2009).
27 T. Shimojima et al., Phys. Rev. Lett. **104**, 057002 (2010).
28 M. Yi et al., Proc. Natl. Acad. Sci. USA **108**, 6878 (2011).
29 S. Aswartham et al., J. Cryst. Growth **314**, 341 (2011).
30 T. Chatterji edt., Neutron Scattering from Magnetic Materials, Elsevier (2006).
31 H. Yamazaki, J. of the Phys. Soc. of Jpn. **32**, 1227 (1972).
32 K. Hirakawa and H.Ikeda, Magnetic Properties of Layered Transition Metal Compound, Kluwer Academics, p. 231 (1990).
33 K. Matan et al., Phys. Rev. B **79**, 054526 (2009).
34 A. Zheludev, ResLib 3.4c (Oak Ridge National Laboratory, Oak Ridge, 2006).
35 D.-X. Yao and E. W. Carlson, Front. Phys. China **5**, 166 (2010).
36 The calculation in reference[35] was done for uniaxial anisotropy, but the case of orthorhombic anisotropy calculated with only nearest-neighbor exchange[31] shows that the two magnon gaps arising from orthorhombic single-ion anisotropy are identical to the two gaps caculated with these parameters in uniaxial anisotropy.
37 A. N. Yaresko et al., Phys. Rev. B **79**, 144421 (2009).
38 J. Knolle et al., Phys. Rev. B **81**, 140506 (2010).
39 E. Kaneshita and T. Tohyama, Phys. Rev. B **82**, 094441 (2010).